Aberrant TGFβ Signalling Contributes to Dysregulation of Sphingolipid Metabolism in Intrauterine Growth Restriction

Sarah Chauvin, Yoav Yinon, Jing Xu, Leonardo Ermini, Julien Sallais, Andrea Tagliaferro, Tullia Todros, Martin Post, and Isabella Caniggia

The Lunenfeld-Tanenbaum Research Institute (S.C., Y.Y., J.X., J.S., A.T., I.C.), Mount Sinai Hospital, Toronto, Canada M5T 3H7; Departments of Obstet Gynecol (Y.Y., I.C.), Physiology (S.C., M.P., I.C.), and Pediatrics (M.P.), Institute of Medical Sciences University of Toronto (M.P., I.C.), Toronto, Canada; The Hospital for Sick Children (L.E., M.P.), Toronto, Canada M5G 1X8; and Department of Obstet Gynecol (T.T.), University of Turin, Turin, Italy 10126

Context: Sphingolipids function as key bioactive mediators that regulate cell fate events in a variety of systems. Disruptions in sphingolipid metabolism characterize several human pathologies.

Objective: In the present study we examined sphingolipid metabolism in intrauterine growth restriction (IUGR), a severe disorder complicating 4–7% of pregnancies at increased risk of perinatal morbidity and mortality, which is characterized by placental dysfunction and augmented trophoblast cell death rates.

Design, Setting, and Participants: Placentae from early severe IUGR with documented abnormal umbilical artery Doppler defined as absence or reverse of end diastolic velocity and a birth weight below the fifth percentile for gestational age were collected (n = 58). Placental tissues obtained from healthy, age-matched preterm and term deliveries (n = 46; TC, n=28) were included as controls.

Results: Sphingolipid analysis by tandem mass spectrometry revealed elevated sphingosine and decreased ceramide levels in placentae from pregnancies complicated by IUGR relative to age-matched controls. Sphingosine accumulation was due to accelerated ceramide breakdown via increased acid ceramidase (ASAH1) expression/activity caused by augmented TGFβ signalling via the ALK5/SMAD2 pathway. In addition, a marked reduction in sphingosine kinase 1 (SPHK1) expression/activity due to impaired TGFβ signalling via ALK1/SMAD1 contributed to the sphingosine buildup in IUGR. Of clinical significance, ALK/SMAD signalling pathways were differentially altered in IUGR placentae.

Conclusions: Altered TGFβ signalling in IUGR placentae causes dysregulation of sphingolipid metabolism, which may contribute to the increased trophoblast cell death typical of this pathology. **(*J Clin Endocrinol Metab* 100: E986–E996, 2015)**

Sphingolipids are ubiquitous components of all eukaryotic cell membranes that, in addition to being structural elements, function as important bioactive mediators in a variety of cell events governing cell death and proliferation (1, 2). At the core of sphingolipid metabolism is ceramide (CER), which is the only sphingolipid that can be synthesized de novo in the endoplasmic reticulum. Once synthesized, CER is transported to a number of subcellular compartments where it can be converted into other sphingolipid species via the action of sphingolipid regulatory

ISSN Print 0021-972X ISSN Online 1945-7197
Printed in USA

Received February 1, 2015. Accepted May 1, 2015.
First Published Online May 5, 2015

Abbreviations: ALK, activin receptor-like kinase; ASAH1, N-acylsphingosine amidohydrolase (acid ceramidase); BMP, bone morphogenic protein; CER, ceramide; IUGR, intrauterine growth restriction; LC MS/MS, liquid chromatography tandem mass spectrometry; PTC, preterm control; S1P, sphingosine-1-phosphate; SPH, sphingosine; SPHK, sphingosine kinase; TC, term control.

enzymes. In the lysosome, acid ceramidase (ASAH1) is responsible for hydrolyzing CER into sphingosine (SPH), which in turn is converted into sphingosine-1-phosphate (S1P) by sphingosine kinases (SPHK1/2). The regulation of the ASAH1/SPHK1 axis is vital for cell homeostasis as S1P promotes cell survival whereas SPH and CER trigger cell death. Heritable deficiencies in ASAH1 activity caused by mutations in the gene encoding the enzyme (*ASAH1*) can result in Farber disease, a lysosomal storage disorder characterized by CER accumulation (3). In contrast, enhanced ASAH1 activity is present in cancers and Alzheimer's disease, thereby decreasing CER levels (3, 4). Similarly, aberrant SPHK1 expression promotes tumorigenesis (5). Consequently, ASAH1 and SPHK1 are critical to maintenance of sphingolipid metabolism as disruptions to their expression/activity can result in serious pathologies.

Early placental development is characterized by a tight coordination of proliferation, differentiation and apoptosis of trophoblast cells. In vitro studies have implicated sphingolipids in trophoblast cell fusion (6), underscoring their importance in the developing placenta. Members of the TGFβ superfamily play key roles in regulating trophoblast cell fate (7–9); however, the interplay between TGFβs and sphingolipid metabolism remains largely unexplored. It has been reported that TGFβ1 reduces CER production of mouse embryonic fibroblast cells, thereby suppressing apoptosis (10). Others have reported a decrease in CER levels in human dermal fibroblasts after TGFβ1 exposure (11) that was accompanied by an augmented expression of SPHK1 leading to S1P accumulation (12). Yet, no information is available on the role of TGFβs in regulating sphingolipid metabolism in the human placenta and its contribution to placental pathology.

Intrauterine growth restriction (IUGR) is a serious complication of pregnancy that is linked to placental insufficiency. Although unanimous agreement over the classification and etiology of IUGR is lacking, IUGR is commonly defined as failure of the fetus to achieve its growth potential and is associated with a birth weight below the 10th percentile for gestational age (13). However; more stringent criteria including fetal weight values below fifth or even third percentile together with measurements of abdominal circumference are often used for IUGR diagnosis and management. IUGR affects approximately 4–7% of births and results in increased risk of perinatal morbidity and mortality (13). Placentae from IUGR pregnancies are characterized by increased trophoblast cell death and impaired trophoblast invasion resulting in inadequate maternal vascular remodelling, leading to poor uteroplacental perfusion and fetal development (14, 15). We have recently reported that sphingolipid metabolism is altered in preeclampsia (16), another pregnancy-related disorder characterized by maternal hypertension. In particular, we show that increased de novo CER synthesis and reduced ASAH1 expression/activity results in CER overload in pre-eclampsia leading to increased trophoblast cell autophagy (16). Although IUGR and preeclampsia share a number of morphological and molecular features suggestive of altered trophoblast cell death rates, the contribution of bioactive sphingolipid mediators to the pathogenesis of IUGR remains to be established. Hence, in the current study, we examined the sphingolipid metabolism in IUGR.

Materials and Methods

Placental tissue collection

Informed consent was obtained from all participants. Tissue collection was performed by the Biobank of Mount Sinai Hospital and by the Sant'Anna Hospital, University of Turin, Italy, in accordance with the Institutions' ethics guidelines. Early gestation placental tissues (5–8 wk gestation; n = 12) were obtained from elective termination of pregnancies. Placental tissue obtained from IUGR pregnancies (n = 58) were selected based on the American College of Obstetricians and Gynaecologists clinical and pathological criteria (13). All women were healthy nonsmokers who did not consume alcohol during pregnancy. Women did not have signs of pre-eclampsia, essential hypertension, infection, or known causes of IUGR including renal, endocrine, and autoimmune disorders. IUGR fetuses exhibited a birth weight below the fifth percentile. Placental tissues collected from healthy, gestational age–matched preterm (PTC, n = 46) and term (TC, n = 28) deliveries with normally grown fetuses that did not have signs of other placental dysfunctions were included as controls. Cervical incompetence, idiopathic labor, and preterm premature rupture of membranes were casual for preterm deliveries. Control and pathological tissues were collected from singleton pregnancy that did not exhibit any fetal anomalies and chromosomal abnormalities. Patients' information, inclusion criteria, and clinical parameters are outlined in Supplemental Table 1.

First trimester villous explant culture

Human villous explant cultures were performed from first trimester human placental tissue (5–8 wk gestation) as previously described (17). For detailed culture and treatments procedures see Supplemental Materials.

Choriocarcinoma cell cultures

Human choriocarcinoma JEG3 cells were seeded at a density of 1.5×10^5 cells per well into six-well plates and cultured in complete EMEM media (ATCC) supplemented with 10% (v/v) heat-inactivated fetal bovine serum at 37°C in standard conditions (5% CO_2 in 95% air) as previously described (14). For detailed culture and treatment conditions see Supplemental Materials.

Transient transfection studies

Smad2 was knocked down in JEG3 cells using a Smad2 siRNA-containing plasmid kindly provided by Dr Chun Peng (York University, Toronto, Canada). For detailed procedures on transfection see Supplemental Materials.

Mass spectral analysis

Placental tissues from IUGR, PTC pregnancies, and villous explants were collected, processed for lipid extraction, and sphingolipidomic analysis was conducted at the Analytical Facility for Bioactive Molecules at The Hospital for Sick Children, Toronto, Canada. Lipid extraction was performed according to Bligh and Dyer (18). Sphingolipids were then analyzed using high-performance liquid chromatography coupled to a tandem mass spectrometer (LC-MS/MS) as previously described (16).

RNA analysis

Total RNA was extracted from frozen placental tissue and JEG3 cells using TRIzol and treated with DNase I to remove genomic DNA contamination. Next, RNA was reverse transcribed using random hexamers (Applied Biosystems) and amplified by PCR. Analysis was performed using the DNA Engine Opticon 2 System (MJ Research) as previously described (19). TaqMan Universal MasterMix and specific TaqMan primers and probes for *ASAH1*, *SPHK1*, and *18S* were purchased from ABI as Assays-on-Demand for human genes. Data were normalized against expression of 18S rRNA using the $2^{-\Delta\Delta Ct}$ formula (19).

Antibodies and Western blot analysis

Western blotting was performed as previously described (19). For details on procedures, reagents, and antibodies used see Supplemental Materials.

Immunohistochemistry and immunofluorescence staining

Immunohistochemical and immunofluorescence analyses were performed in tissue sections from IUGR and PTC as previously described (8, 14).

ASAH1 and SPHK1 activity measurements

ASAH1 activity was measured as described previously (16). SPHK1 activity was assessed using an Echelon SPHK1 Assay Kit (K-3500) according to the manufacturer's protocol (Echlon Bioscience).

Statistical analysis

Statistical analysis was performed using GraphPad Prism 4 software. For comparison of two groups an unpaired *t* test was used with or without Welch's correction, where applicable. For comparison between multiple groups, one-way ANOVA with post-hoc Student-Newman-Keuls test was performed or two-way ANOVA with post-hoc Bonferroni test, where applicable. Statistical significance was defined as $P < .05$ and results are expressed as the mean ± SEM.

Results

Ceramide metabolism is disrupted in IUGR pregnancies

We first measured sphingolipid levels in placental tissue from IUGR pregnancies and PTC using LC-MS/MS. Characteristics of the study population are summarized in Supplemental Table 1. Lipidomic analyses revealed significantly decreased levels in ceramide species C18-Cer(d18:1/18:0), C20-Cer(d18:1/20:0), and C24-Cer(d18:1/24:0) in IUGR placentae relative to PTC (Figure 1A). No changes in C16-Cer(d18:1/16:0) levels were observed between groups. Tissue CER levels are maintained by a balance between their rates of synthesis and breakdown, which is highly dependent on the activity of specific enzymes. Sphinganine and dihydrocreamide (eg, DHcerC24) levels (de novo-precursors of ceramides) were increased in IUGR (Supplemental Figure 1) suggesting an increase in de novo ceramide pathway. This observation together with the decreased CER levels is highly suggestive of enhanced CER turnover in IUGR placentae. Given that total sphingomyelin levels did not change in IUGR vs PTC placentae (Supplemental Figure 1), we postulated that an increased degradation of CER by ASAH1 and not an increased conversion of sphingomyelin into CER via sphingomyelinase was responsible for the reduced CER levels. ASAH1 is synthesized as a 55-kDa precursor protein that undergoes autoproteolytic cleavage in the lysosome, producing a 53-kDa dimeric active form (20). Western blot analysis of human placental lysates identified ASAH1 as a band with a molecular mass of 40 kDa, corresponding to the molecular weight of the β-subunit of the active enzyme (Figure 1, B and C). Specificity of the ASAH1 antibody was validated using a blocking peptide (Figure 1B). In agreement with decreased CER levels in IUGR, we found augmented ASAH1 protein levels in IUGR placentae relative to PTC (Figure 1C), as well as increased ASAH1 activity (Figure 1D). It should be noted that labor, gestation, and sex did not affect placental ASAH1 protein expression (Supplemental Figure 2, A and B). Immunohistochemical staining revealed strong positive ASAH1 signal in the trophoblast layer of IUGR placentae (Figure 1E). Low positive immunoreactivity was observed in PTC sections, whereas no signal was detected in nonimmune IgG control. Collectively, these findings suggest enhanced breakdown of CER to sphingosine by ASAH1 in IUGR placentae.

Signalling via ALK5 regulates ASAH1 expression

IUGR is characterized by sustained placental hypoxia and elevated TGFβ expression, which contributes to the placental dysfunction typical of this pathology (15, 21). Hence, we examined the effect of TGFβ on ASAH1 expression in human choriocarcinoma JEG3 cells, an established in vitro model of placental origin. Exposure of JEG3 cells to either 5 ng/mL TGFβ1 or β3 for 3 and 8 hours significantly increased *ASAH1* mRNA

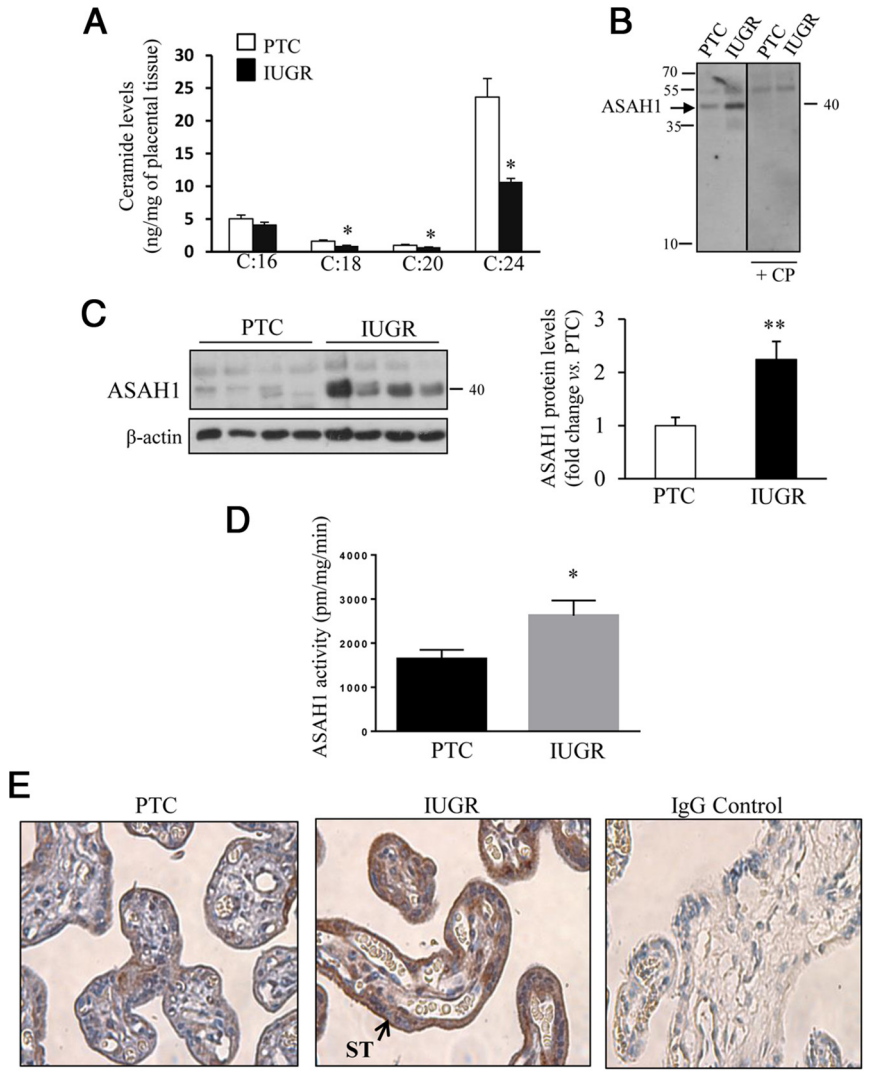

Figure 1. Ceramide levels and ASAH1 expression are altered in placentae from IUGR pregnancies. A, CER levels measured by LC-MS/MS in placental tissue from IUGR pregnancies compared with age-matched preterm controls (PTC). Numbers indicate the number of carbons in the fatty acid chain bound to sphingosine (d18:1) backbone (IUGR, n = 33; PTC, n = 23; *, $P < .05$). B, Western blot analysis of human placental tissue identified ASAH1 as a band of 40 kDa. Incubation with a blocking peptide selectively competed for the 40 kDa band. C, Representative immunoblot showing ASAH1 expression in IUGR placentae compared with PTC placentae. C, (Right panel) densitometric analysis of ASAH1 protein expression in IUGR and PTC placentae normalized to β-actin and expressed as a fold change relative to PTC (IUGR, n = 14; PTC, n = 11, **, $P < .01$). D, ASAH1 activity in IUGR vs PTC placentae (IUGR, n = 6; PTC, n = 6; *, $P < .05$). E, ASAH1 spatial localization in IUGR and PTC placental sections (IUGR, n = 3; PTC, n = 3). Images are shown at 40× magnifications. Negative IgG; ST, syncytiotrophblast.

levels (Figure 2A). ASAH1 protein levels were also markedly increased in JEG3 cells following a 24-hour exposure to TGFβ1 or β3 (Figure 2B).

Classical TGFβ signalling is initiated by TGFβ binding to a type II serine threonine kinase receptor that subsequently recruits and phosphorylates activin receptor-like kinase 5 (ALK5), leading to SMAD2/3 activation (22). To determine whether ALK5/SMAD2 signalling was responsible for mediating the TGFβ effect on ASAH1 expression, we treated JEG3 cells with 5μM SB431542, an inhibitor that selectively blocks ALK5 signalling. SB431542 treatment indeed reversed the TGFβ1 and β3 stimulatory effect on ASAH1 protein expression (Figure 2C). To confirm that SB431542 acted as an ALK5 inhibitor we measured SMAD2 phosphorylation after TGFβ1 and β3 stimulation. SB431542 treatment entirely abrogated TGFβ1/3-induced SMAD2 phosphorylation (Figure 2C) while total SMAD2 levels remained unchanged (Figure 2C). We then knocked down SMAD2 expression by transiently transfecting JEG3 cells with either empty vector (pSuper) or a plasmid encoding SMAD2 siRNA. Consistent with the SB431542 results, TGFβ-induced expression of ASAH1 was significantly reduced in siSMAD2-transfected cells relative to control empty vector (Figure 2D). Expectedly, pSMAD2 expression was decreased in siSMAD2-transfected cells (Figure 2D).

Having demonstrated a TGFβ/ALK5-mediated effect on ASAH1 expression in JEG3 cells, we next assessed the role of TGFβ1/3 in regulating ASAH1 expression in human villous explants, a well-established ex vivo placental model (17). Given that TGFβ1 and β3 are highly expressed in the human placenta during early gestation (8, 23), we reasoned that blocking ALK5 signalling with SB431542 would be a suitable experimental approach. Exposure of villous explants to SB431542 inhibited ALK5 signalling as demonstrated by reduced pSMAD2 and ASAH1 expression compared with control vehicle-treated explants (Figure 2E). To establish whether the reduction in ASAH1 levels in SB431542-treated villous explants would affect CER turnover we also measured CER levels. We observed significant increases in C18-Cer(d18:1/18:0), C20-Cer(d18:1/20:0), and C24-Cer(d18:1/24:0) in SB431542-treated explants relative to controls (Figure 2F). Collectively, these data are in support of the TGFβ/ALK5/SMAD2 pathway regulating CER levels via ASAH1 in the human placenta.

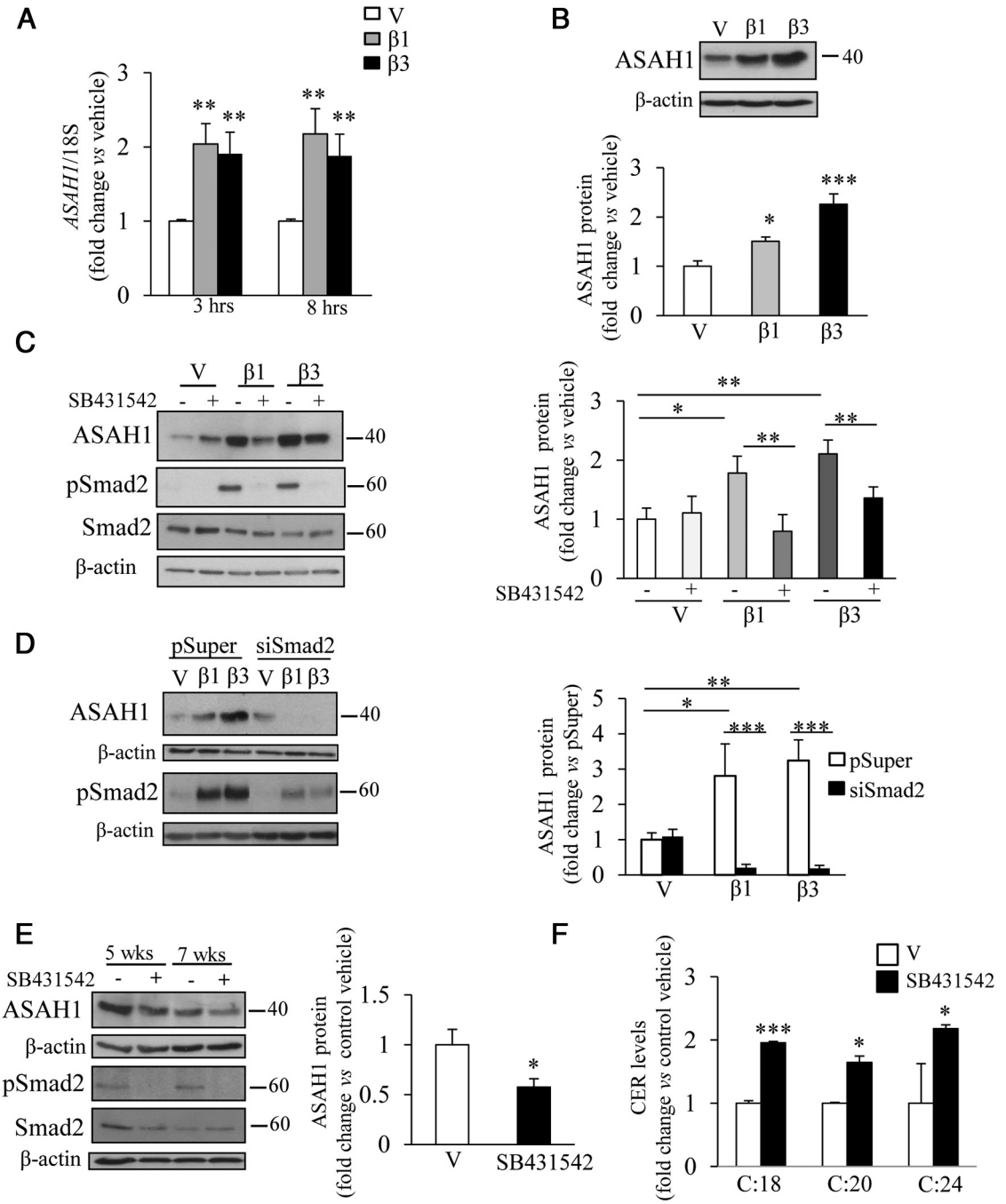

Figure 2. TGFβ1 or β3 treatment increases ASAH1 expression in an ALK5/Smad2-dependent manner in JEG3 cells and in villous explants. A, *ASAH1* mRNA expression in JEG3 cells treated with 5 ng/mL TGFβ1 or β3 relative to control vehicle (V) (n = 3; **, $P < .01$). B, (Upper panel) representative immunoblot for ASAH1 in JEG3 cells following 24-h exposure to TGFβ1, TGFβ3, or control vehicle (V). B, (Bottom panel) densitometric analysis of ASAH1 protein expression in TGFβ1/3-treated JEG3 cells. Data are expressed as a fold change relative to control (V) vehicle (n = 8; *, $P < .05$; **, $P < .01$; and ***, $P < .001$). C, (Right panel) representative immunoblot for ASAH1, pSMAD2, and SMAD2 expression in TGFβ1/3-treated JEG3 relative to control vehicle in the presence or absence of ALK5-inhibitior SB431542 (5μM). C, (Left panel) densitometric analysis of ASAH1 protein expression in TGFβ1/3-treated JEG3 cells in the presence or absence of SB431542. Data are expressed as a fold change relative to control vehicle (V) (n = 3; *, $P < .05$; **, $P < .01$). D, Representative immunoblot of ASAH1, pSMAD2 protein expression in pSuper- and siSMAD2-transfected JEG3 cells treated with control vehicle (V) or TGFβ1/3. D, (Right panel) densitometric analysis of ASAH1 protein levels in siSMAD2-transfected JEG3 cells normalized to ACTB and expressed as a fold change relative to control vehicle (V) (n = 3; *, $P < .05$, **, $P < .01$; ***, $P < .001$). E, (Right panel) representative immunoblot showing ASAH1, pSMAD2, and total SMAD2 expression in villous explants treated with control vehicle (V) or ALK5 inhibitor SB431542 (10μM). E, (Left panel) densitometric analysis of ASAH1 protein expression in SB431542-treated villous explants normalized to ACTB and expressed as a fold change relative to control vehicle (V) treatment (n = 5 explants; *, $P < .05$). F, Ceramide levels measured by LC-MS/MS in human villous explants following SB431542 treatment, expressed as a fold change relative to control vehicle (V) (n = 5 explants; *, $P < .05$; ***, $P < .001$).

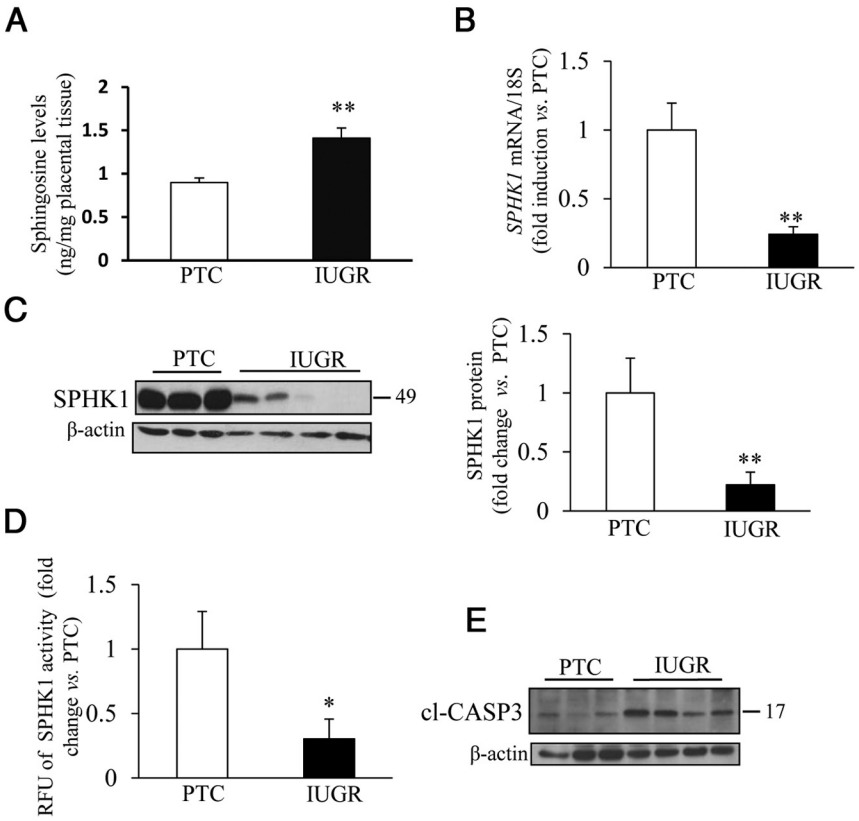

Figure 3. Sphingosine levels and SPHK1 expression are altered in placentae from IUGR pregnancies. A, Sphingosine levels measured by LC-MS/MS in placental tissue from IUGR and PTC pregnancies (IUGR, n = 26; PTC, n = 17; *, $P < .05$). B, *SPHK1* mRNA expression in placentae from IUGR relative to PTC pregnancies as determined by qPCR (IUGR, n = 10; PTC, n = 9; **, $P < .01$). C, SPHK1 protein expression in IUGR relative to PTC placentae (IUGR, n = 14; PTC, n = 11; **, $P < .01$). D, SPHK1 activity in IUGR placentae compared with PTC placentae expressed as a fold change relative to PTC (IUGR = 10; PTC = 5; *, $P < .05$). E, Cleaved caspase 3 (cl-CASP3) protein expression in placentae from IUGR relative to PTC pregnancies.

Sphingosine metabolism is disrupted in IUGR pregnancies

In line with increased ASAH1 expression/activity and decreased CER levels in IUGR, sphingosine (SPH) levels were significantly increased in IUGR compared with PTC placentae (Figure 3A). Given that sphingosine can be further modified by SPHK to produce S1P we next examined SPHK1 expression. Real-time PCR revealed a marked decrease in *SPHK1* mRNA levels in IUGR vs PTC placentae (Figure 3B). Western blotting of human placental lysates identified SPHK1 as a single band at 49 kDa. In agreement with mRNA findings, SPHK1 protein levels were markedly decreased in IUGR placentae (Figure 3C) and this was accompanied by a significant decrease in SPHK1 activity (Figure 3D). Labor, gestation, and sex did not affect SPHK1 expression (Supplemental Figure 2). Thus, SPHK1 expression and activity are markedly reduced in IUGR placentae independent of mode of delivery, gestation, and fetal sex, thereby contributing to the accumulation of SPH. SPH is a known inducer of apoptosis (24); hence, it is plausible that elevated SPH seen in IUGR may contribute to increased placental cell death found in IUGR. Cleaved-caspase3 analysis confirmed the augmented levels of apoptotic cell death in IUGR placentae (Figure 3E).

Signalling via ALK1 regulates SPHK1 expression

To determine whether, similarly to ASAH1, altered TGFβ signalling contributes to impaired SPHK1 expression in IUGR, JEG3 cells were exposed to either TGFβ1 or β3. Real-time PCR and Western blotting demonstrated that TGFβ1 or β3-treated JEG3 cells had significantly reduced *SPHK1* mRNA and protein levels compared with control vehicle-treated cells (Figure 4A, B). Although TGFβ-induced SMAD2 phosphorylation in JEG3 cells was inhibited by SB431542, ALK5 inhibition by SB431542 did not reverse the negative effect of TGFβ1/3 on SPHK1 expression (Supplemental Figure 3A). Knockdown of SMAD2 expression with SMAD2 siRNA did also not reverse the TGFβ3 (and to a lesser extent TGFβ1) induced reduction of SPHK1 in JEG3 cells (Supplemental Figure 3B). To further rule out ALK5 signalling in regulating placental SPHK1 levels we examined SPHK1 expression in villous explants following SB431542 treatment. Western blotting revealed reduced SMAD2 phosphorylation following SB431542 treatment, but no significant changes in SPHK1 expression (Supplemental Figure 3C). In addition, no differences in SPH levels in SB431542-treated vs control vehicle–treated explants were observed (Supplemental Figure 3D). Thus, in contrast with ASAH1, the ALK5/SMAD2 pathway seems not to mediate the effect of TGFβ on SPHK1 expression.

TGFβs have also been shown to activate another type 1 receptor/SMAD pathway (25), namely ALK1 that induces SMAD1/5 phosphorylation. Hence, JEG3 cells were exposed to TGFβ1/3 in the presence or absence of 10μM of the ALK1 inhibitor dorsomorphin. Surprisingly, dorsomorphin inhibited pSMAD1 phosphorylation as well as SPHK1 expression in unstimulated cells, suggesting that ALK1 signalling is crucial for maintaining basal SPHK1 expression (Figure 4C). Exposure of JEG3 cells to TGFβ1/3 stimulated

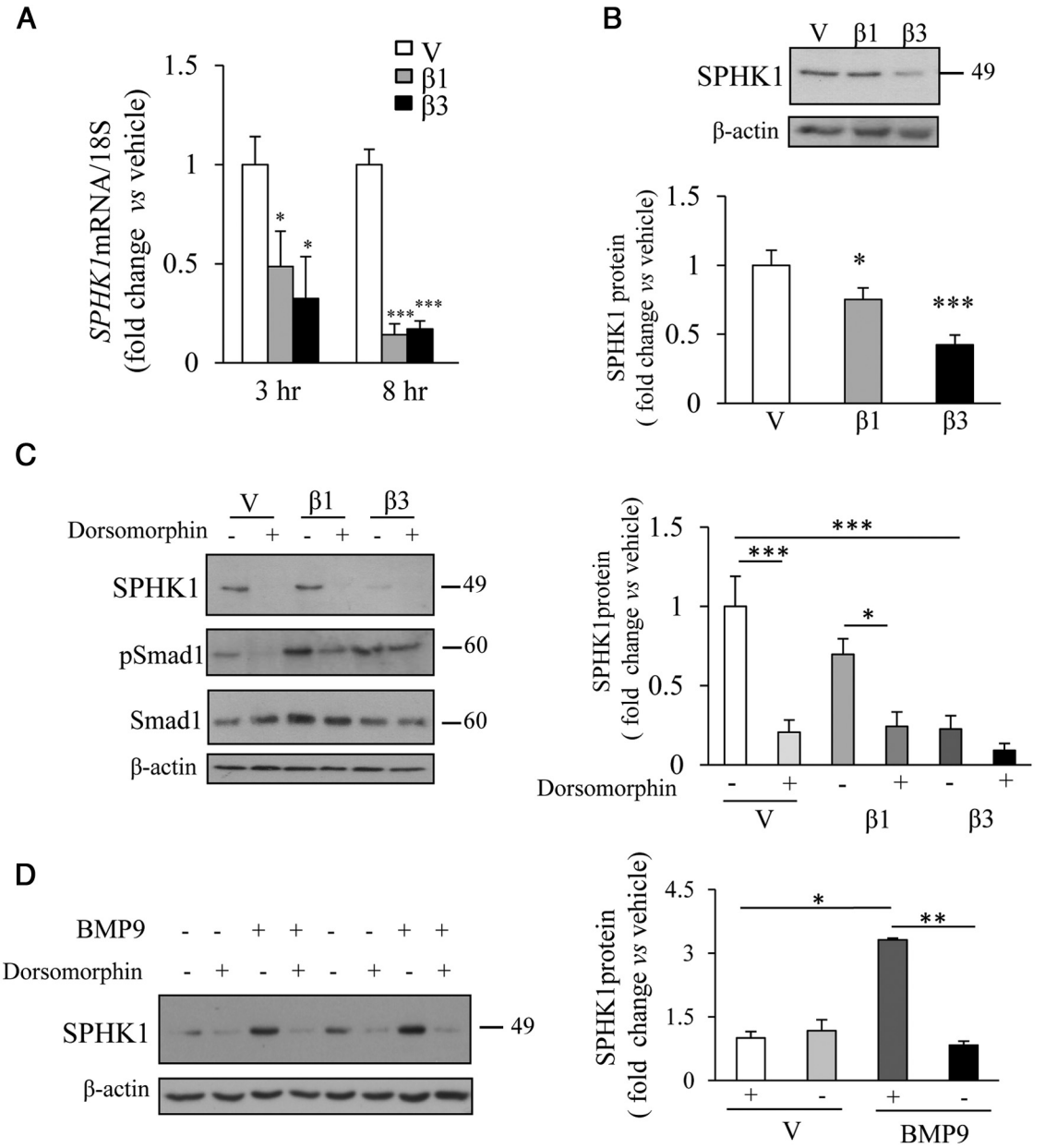

Figure 4. TGFβ3 reduces SPHK1 expression in JEG3 via ALK1, but not ALK5 signalling. A, *SPHK1* mRNA levels in JEG3 cells following 5 ng/mL TGFβ1/3 treatment relative to control vehicle (V) as measured by qPCR (n = 4; *, $P < .05$; ***, $P < .001$). B, SPHK1 protein levels in TGFβ1/3 and control vehicle (V)-treated JEG3 cells (upper panel) (n = 9; *, $P < .05$; ***, $P < .001$). C, Representative immunoblots for SPHK1, pSMAD1, and total SMAD1 expression in TGFβ1/3- and control vehicle (V)-treated JEG3 cells in the presence or absence of the ALK1 inhibitor 10μM Dorsomorphin. C, (Right panel) densitometric analysis of SPHK1 protein expression in TGFβ1/3-treated JEG3 cells in the absence or presence of Dorsomorphin normalized to ACTB and expressed as a fold change relative to control (V) vehicle (n = 3; *, $P < .05$; ***, $P < .001$). D, Representative immunoblot and densitometric analysis for SPHK1 in BMP9 treated JEG3 cells in the presence or absence of Dorsomorphin (n = 3; *, $P < .05$; ***, $P < .001$).

SMAD1 phosphorylation that was reduced by dorsomorphin (Figure 4C), indicating that ALK1 signalling is activated by TGFβ1/3. However, dorsomorphin did not reverse the negative effect of TGFβ3 on SPHK1 expression. In contrast, SPHK1 expression was further reduced in both TGFβ1/3 plus dorsomorphin groups compared with TGFβ1/3 alone (Figure 4C). These data suggest that TGFβ opposes positive ALK1 signalling toward SPHK1 expression. To confirm ALK1-positive signalling toward SPHK1 expression we treated JEG3 cells with bone morphogenic protein 9 (BMP9), a ligand that binds with high affinity to ALK1 (26). BMP9 increased SPHK1 expression that was abrogated by dorsomorphin (Figure 4D), underscoring positive ALK1 signalling in controlling SPHK1 expression. To rule out other TGFβ-stimulated signalling pathways we repeated similar experiments with pharmacological inhibitors (U0126, SN239063, and SP600125) of MAPK/ERK, p38MAPK, and JNK/MAPK, respectively. None of the inhibitors reversed the TGFβ-induced reduction in SPHK1 expression (Supplemental Figure 3E).

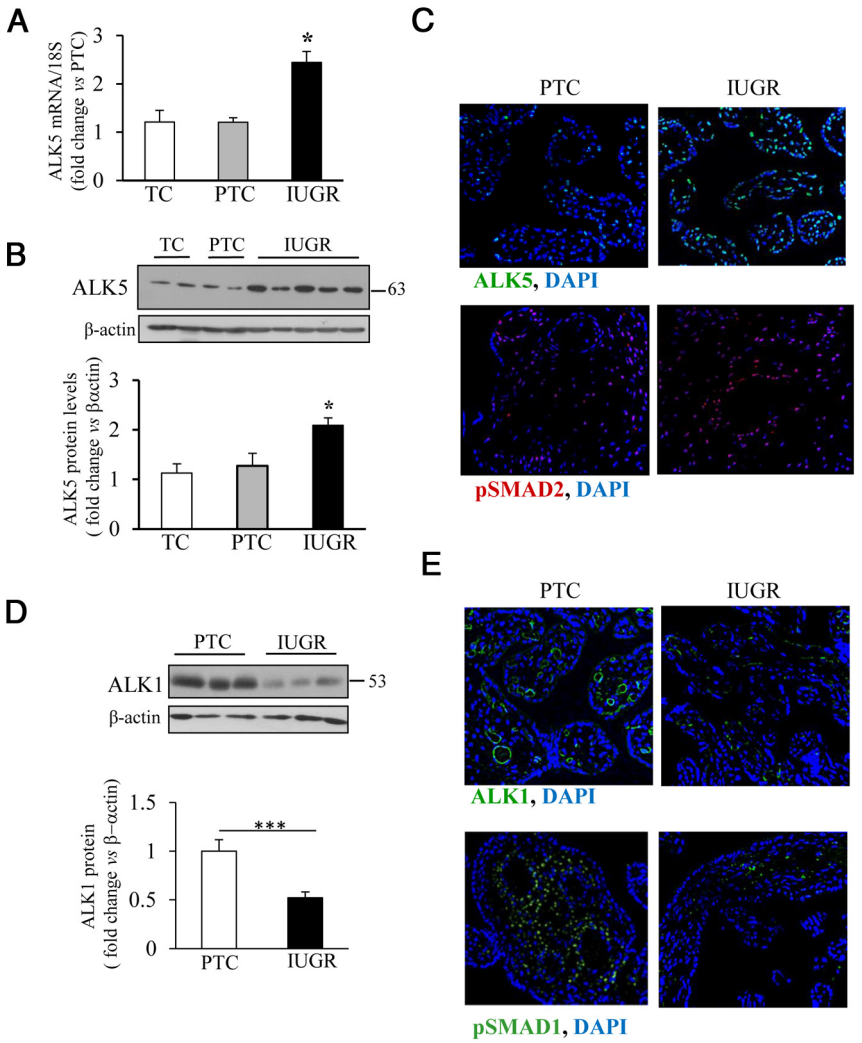

Figure 5. ALK5/pSmad2 and ALK1/pSmad1 are differentially expressed in placentae from IUGR pregnancies. A, *ALK5* mRNA levels in IUGR placentae compared with PTC and TC placental tissue normalized to *18S* and expressed as a fold change relative TC as detected by qPCR (TC, n = 4; PTC, n = 8; IUGR, n = 10; *, $P < .05$). B, ALK5 protein expression in IUGR placentae compared with PTC and TC (IUGR, n = 22; PTC, n = 12; TC, n = 10; *, $P < .05$). C, Representative immunofluorescence images for ALK5 and pSMAD2 in IUGR and PTC placental tissue sections. D, ALK1 protein expression levels in IUGR and PTC placentae. E, Representative immunofluorescence images for ALK1 and pSMAD1 in placental tissue sections from IUGR and PTC. Images are shown at 40× magnification.

Changes in ALK1 and ALK5 expression in IUGR placentae

We next examined ALK5/pSMAD2 and ALK1/pSMAD1 expression in IUGR placentae. We found increased ALK5 mRNA and protein levels in IUGR placentae when compared with PTCs and TCs (Figure 5A, B). Immunofluorescence staining showed strong positive ALK5 and pSMAD2 immunoreactivity primarily in the trophoblast layer of placental villi from IUGR pregnancies (Figure 5C), suggesting increased activation of ALK5-mediated TGFβ signalling in IUGR (Figure 5C, lower panel). In stark contrast, ALK1 protein levels were markedly decreased in IUGR placentae relative to controls (Figure 5D). Immunofluorescence staining corroborated the reduction of ALK1 and its downstream signal pSMAD1 in IUGR placentae compared with PTC. Intriguingly, their expression was mainly restricted to chorionic vessels (Figure 5E).

Discussion

Bioactive sphingolipids are key regulators of cell fate events during organogenesis and in disease status. In the present study, we report that alteration in ASAH1 and SPHK1 expression and activity tilts the SPH/S1P balance toward prodeath SPH in placentae from severely IUGR pregnancies. Using human villous explants and human choriocarcinoma JEG3 cells we further demonstrate that TGFβ1/3 are primarily responsible for regulating ASAH1 and SPHK1 expression via distinct ALK/SMAD-signalling pathways. TGFβ1/3 signals via ALK5/SMAD2 to induce ASAH1 protein expression, whereas positive ALK1/ALK5/SMAD1 signaling toward SPHK1 is opposed by TGFβ1/3. Of clinical significance, we report differentially altered ALK/SMAD signal pathways in IUGR that contribute to the impaired placental sphingolipid metabolism found in this pathology.

Changes in the expression/activity of sphingolipid metabolizing enzymes that result in lipid accumulation are common to a number of human pathologies including lysosomal storage disorders, and cancers (27). Similar to IUGR placentae, increased ASAH1 expression/activity has been reported in human prostate cancer and melanomas (28, 29). The enhanced CER degradation by elevated ASAH1 expression/activity in IUGR placentae is in stark contrast with preeclampsia where deficient ASAH1 expression/activity leads to increased CER levels (16). These distinctive sphingolipid signatures are not surprising given that preeclampsia and IUGR represent placental disorders with different trophoblast cell phenotypes (14, 30).

Breakdown of CER by ASAH1 is required for SPH production that, in turn, is phosphorylated to prosurvival S1P by SPHK1. In vitro studies with murine fibrosarcoma cells

have shown that elevated ASAH1 lead to reduced ceramide levels as well as suppression of apoptosis (31). Similar to cancer cells, enhanced CER degradation via increased ASAH1 expression/activity in IUGR placentae implies an adaptive mechanism aimed at maintaining proper trophoblast cell homeostasis. However, SPH conversion into S1P in IUGR placentae is prevented by a marked reduction in SPHK1 expression/activity. In contrast with prosurvival S1P, SPH is a potent cell death inducer (24). Although CER overload is responsible for increased trophoblast cell death in preeclampsia (16), it is plausible that SPH accumulation in IUGR in part accounts for elevated trophoblast cell death rates seen in this disease (Figure 3E). Thus, disrupted sphingolipid metabolism may differentially contribute to improper placentation typical of these pathologies.

SPHK is a highly conserved enzyme that exists in two isoforms, SPHK1 and SPHK2. SPHK1 is expressed and functions in the cytosol, whereas SPHK2 expression is restricted to the nucleus (32). SPHK1 is involved in promoting cell survival, angiogenesis, and tumorigenesis (33). During pregnancy, uterine SPHK1 expression is thought to mediate growth and differentiation of uterine tissues (34) and SPHK1 gene disruptions causes defective decidualization (34). In addition, female homozygous knockouts for *SPHK1* have a massive uterine accumulation of SPH (35). These pregnancy-related phenotypic findings in defective *SPHK1* rodent models agree with our data in humans, suggesting that an altered sphingolipid metabolism may contribute to placental insufficiency typical of IUGR.

Proinflammatory cytokines, growth factors, and oxidative stress have been shown to impinge on the sphingolipid rheostat (36). To date only a handful of reports have shown TGFβ regulation of sphingolipid metabolism; however, none of these studies have examined the placenta. To our knowledge we are the first to report a TGFβ-mediated regulation of ASAH1 expression in trophoblast cells or any other cell types for that matter. Sato et al (11) reported decreased CER levels following TGFβ1 treatment of serum-starved fibroblasts; however, they did not examine whether this was due to changes in ASAH1 expression/activity. Our data strongly suggest that TGFβ1/3 signalling via ALK5/SMAD2 increases ASAH1 expression resulting in augmented conversion of CER into SPH.

Reports have shown that TGFβ1 up-regulates SPHK1 expression and activity, thereby protecting cells from apoptosis (12, 36, 37). In contrast, we observed a marked decrease in SPHK1 following exposure to TGFβ3, but less with TGFβ1. No studies have ascribed a role for TGFβ3 in sphingolipid metabolism; yet, in the present study, TGFβ3 had the most profound effect on both ASAH1 and SPHK1 expression in JEG3 cells. Although TGFβ isoforms share overlapping functions, TGFβ3 has been shown to be an important regulator of human placentation (8). This unique role for TGFβ3 in trophoblast differentiation may explain why we observed a more profound effect on sphingolipid metabolizing enzymes with TGFβ3 than TGFβ1.

Herein, we found that inhibition of canonical ALK5-mediated signalling had no effect on SPHK1 expression but that selective blocking of ALK1 activity with dorsomorphin negatively affect SPHK1 expression and function. Studies using endothelial cells have identified ALK1 as an additional type I TGFβ receptor, which requires ALK5 for its function (38). Although ALK5 activates SMAD2/3, TGFβ activation of ALK1 leads to phosphorylation of BMP-mediated SMAD1/5 (38). It seems that ALK5 and ALK1 are not redundant, but rather activate different SMAD-mediated signalling pathways that promote angiogenesis (39). Interestingly, S1P, the product of SPHK1, is proangiogenic. Hence, reduced ALK1 expression, specifically in the chorionic vessels, together with negative TGFβ3 signaling resulting in diminished SPHK1 expression in IUGR may explain the impaired SPH processing to S1P, which may result in the hypovascular phenotype typical of this pathology. Mutations of the *ALK1* gene have been linked to the type II hereditary hemorrhagic telangiectasia, a disorder characterized by multi-

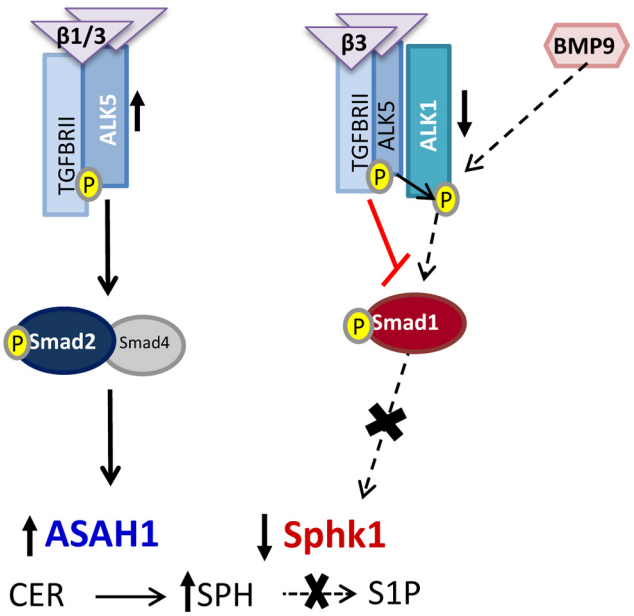

Figure 6. Putative model of TGFβ-mediated regulation of ASAH1 and SPHK1 expression in IUGR. Canonical TGFβ signalling involves TGFβ binding to a TGFβ Receptor II and activin receptor-like kinase 5 (ALK5) or ALK1, which in turn phosphorylate and activate distinct intracellular SMAD proteins that regulate gene expression. In IUGR elevated ALK5 signalling via SMAD2 increases ASAH1 expression leading to augmented CER conversion to SPH. Moreover, deficient ALK1 signalling via SMAD1 and its inhibition by TGFβ3 suppresses SPHK1 expression; thereby further contributing to SPH accumulation in IUGR.

systemic vascular dysplasia, indicating that ALK1 may mediate signals important for the formation or remodeling of blood vessels (40, 41). Others have reported that *ALK1*-deficient mice embryos die at mid gestation due to severe vascular abnormalities and that disruption of *ALK1* leads to dominance of the ALK5 signalling pathway (38). These studies and our findings support the idea that an imbalance in ALK1 and ALK5 signalling in the IUGR placenta impairs angiogenesis that in part may be due to a changed sphingolipid rheostat.

In conclusion, our results suggest that alterations in expression of the sphingolipid regulatory enzymes ASAH1 and SPHK1 in IUGR placentae is governed by TGFβ3 via different signalling pathways (Figure 6), thereby leading to accumulation of prodeath SPH and consequently, contributing to the enhanced cell death and abnormal angiogenesis, seen in this disorder.

Acknowledgments

We thank the BioBank Program, the Lunenfeld-Tanenbaum Research Institute, and the MSH Department of Obstetrics & Gynaecology for the human specimens used in this study.

Address all correspondence and requests for reprints to: Isabella Caniggia, MD, PhD, Mount Sinai Hospital, Lunenfeld-Tanenbaum Research Institute, 25 Orde Street, Room 6-1004, Toronto, ON, Canada M5T 3H7. E-mail: caniggia@lunenfeld.ca.

This work was supported by the Canadian Institutes of Health Research (CIHR) Grant MOP-14096 (to I.C.) and Canadian Foundation of Innovation (CFI) grant (to M.P.). S.C. was the recipient of a Scholarship from OGS. M.P. is the holder of a Canadian Research Chair in Fetal, Neonatal, and Maternal Health.

Disclosure Summary: The authors have nothing to disclose.

References

1. **Hannun YA, Obeid LM.** Principles of bioactive lipid signalling: Lessons from sphingolipids. *Nat Rev Mol Cell Biol*. 2008;9:139–150.
2. **Hannun YA, Bell RM.** Functions of sphingolipids and sphingolipid breakdown products in cellular regulation. *Science*. 1989;243:500–507.
3. **Park JH, Schuchman EH.** Acid ceramidase and human disease. *Biochim Biophys Acta*. 2006;1758:2133–2138.
4. **Hla T, Dannenberg AJ.** Sphingolipid signaling in metabolic disorders. *Cell Metabol*. 2012;16:420–434.
5. **Pyne NJ, Pyne S.** Sphingosine 1-phosphate and cancer. *Nat Rev Cancer*. 2010;10:489–503.
6. **Singh AT, Dharmarajan A, Aye IL, Keelan JA.** Ceramide biosynthesis and metabolism in trophoblast syncytialization. *Mol Cell Endocrinol*. 2012;362:48–59.
7. **Graham CH, Lysiak JJ, McCrae KR, Lala PK.** Localization of transforming growth factor-beta at the human fetal-maternal interface: Role in trophoblast growth and differentiation. *Biol Reprod*. 1992;46:561–572.
8. **Caniggia I, Grisaru-Gravnosky S, Kuliszewsky M, Post M, Lye SJ.** Inhibition of TGF-beta 3 restores the invasive capability of extravillous trophoblasts in preeclamptic pregnancies. *J Clin Invest*. 1999;103:1641–1650.
9. **Caniggia I, Winter JL.** Adriana and Luisa Castellucci Award lecture 2001. Hypoxia inducible factor-1: Oxygen regulation of trophoblast differentiation in normal and pre-eclamptic pregnancies—A review. *Placenta*. 2002;23 Suppl A:S47–S57.
10. **Chen HH, Zhao S, Song JG.** TGF-beta1 suppresses apoptosis via differential regulation of MAP kinases and ceramide production. *Cell Death Differ*. 2003;10:516–527.
11. **Sato M, Markiewicz M, Yamanaka M, et al.** Modulation of transforming growth factor-beta (TGF-beta) signaling by endogenous sphingolipid mediators. *J Biol Chem*. 2003;278:9276–9282.
12. **Yamanaka M, Shegogue D, Pei H, et al.** Sphingosine kinase 1 (SPHK1) is induced by transforming growth factor-beta and mediates TIMP-1 up-regulation. *J Biol Chem*. 2004;279:53994–54001.
13. **American College of Obstetricians and Gynecologists.** ACOG Practice bulletin no. 134: Fetal growth restriction. *Obstet Gynecol*. 2013;121:1122–1133.
14. **Rolfo A, Garcia J, Todros T, Post M, Caniggia I.** The double life of MULE in preeclamptic and IUGR placentae. *Cell Death Dis*. 2012;3:e305.
15. **Yinon Y, Nevo O, Xu J, et al.** Severe intrauterine growth restriction pregnancies have increased placental endoglin levels: Hypoxic regulation via transforming growth factor-beta 3. *Am J Pathol*. 2008;172:77–85.
16. **Melland-Smith M, Ermini L, Chauvin S, et al.** Disruption of sphingolipid metabolism augments ceramide-induced autophagy in preeclampsia. *Autophagy*. 2015;4:653–669.
17. **Caniggia I, Taylor CV, Ritchie JW, Lye SJ, Letarte M.** Endoglin regulates trophoblast differentiation along the invasive pathway in human placental villous explants. *Endocrinology*. 1997;138:4977–4988.
18. **Bligh EG, Dyer WJ.** A rapid method of total lipid extraction and purification. *Can J Biochem Physiol*. 1959;37:911–917.
19. **Soleymanlou N, Wu Y, Wang JX, et al.** A novel Mtd splice isoform is responsible for trophoblast cell death in pre-eclampsia. *Cell Death Differ*. 2005;12:441–452.
20. **Ferlinz K, Kopal G, Bernardo K, et al.** Human acid ceramidase: Processing, glycosylation, and lysosomal targeting. *J Biol Chem*. 2001;276:35352–35360.
21. **Nevo O, Many A, Xu J, et al.** Placental expression of soluble fms-like tyrosine kinase 1 is increased in singletons and twin pregnancies with intrauterine growth restriction. *J Clin Endocrinol Metab*. 2008;93:285–292.
22. **Kretzschmar M, Massagué J.** SMADs: Mediators and regulators of TGF-beta signaling. *Curr Opin Genet Dev*. 1998;8:103–111.
23. **Ietta F, Wu Y, Winter J, et al.** Dynamic HIF1A regulation during human placental development. *Biol Reprod*. 2006;75:112–121.
24. **Ullio C, Casas J, Brunk UT, et al.** Sphingosine mediates TNFα-induced lysosomal membrane permeabilization and ensuing programmed cell death in hepatoma cells. *J Lipid Res*. 2012;53:1134–1143.
25. **Goumans MJ, Valdimarsdottir G, Itoh S, Rosendahl A, Sideras P, ten Dijke P.** Balancing the activation state of the endothelium via two distinct TGF-beta type I receptors. *EMBO J*. 2002;21:1743–1753.
26. **Chen YG, Massagué J.** Smad1 recognition and activation by the ALK1 group of transforming growth factor-beta family receptors. *J Biol Chem*. 1999;274:3672–3677.
27. **Schulze H, Sandhoff K.** Lysosomal lipid storage diseases. *Cold Spring Harb Perspect Biol*. 20111;3(6):a004804.
28. **Seelan RS, Qian C, Yokomizo A, Bostwick DG, Smith DI, Liu W.** Human acid ceramidase is overexpressed but not mutated in prostate cancer. *Genes Chromosomes Cancer*. 2000;29:137–146.
29. **Musumarra G, Barresi V, Condorelli DF, Scirè S.** A bioinformatic approach to the identification of candidate genes for the development of new cancer diagnostics. *Biol Chem*. 2003;384:321–327.
30. **Newhouse SM, Davidge ST, Winkler-Lowen B, Demianczuk N,**

Guilbert LJ. In vitro differentiation of villous trophoblasts from pregnancies complicated by intrauterine growth restriction with and without pre-eclampsia. *Placenta*. 2007;28:999–1003.

31. **Strelow A, Bernardo K, Adam-Klages S, et al.** Overexpression of acid ceramidase protects from tumor necrosis factor-induced cell death. *J Exp Med*. 2000;192:601–612.
32. **Maceyka M, Sankala H, Hait NC, et al.** SphK1 and SphK2, sphingosine kinase isoenzymes with opposing functions in sphingolipid metabolism. *J Biol Chem*. 2005;280:37118–37129.
33. **Gude DR, Alvarez SE, Paugh SW, et al.** Apoptosis induces expression of sphingosine kinase 1 to release sphingosine-1-phosphate as a "come-and-get-me" signal. *FASEB J*. 2008;22:2629–2638.
34. **Jeng YJ, Suarez VR, Izban MG, Wang HQ, Soloff MS.** Progesterone-induced sphingosine kinase-1 expression in the rat uterus during pregnancy and signaling consequences. *Am J Physiol Endocrinol Metab*. 2007;292:E1110–1121.
35. **Mizugishi K, Li C, Olivera A, et al.** Maternal disturbance in activated sphingolipid metabolism causes pregnancy loss in mice. *J Clin Invest*. 2007;117:2993–3006.
36. **Lebman DA, Spiegel S.** Cross-talk at the crossroads of sphingosine-1-phosphate, growth factors, and cytokine signaling. *J Lipid Res*. 2008;49:1388–1394.
37. **Gellings Lowe N, Swaney JS, Moreno KM, Sabbadini RA.** Sphingosine-1-phosphate and sphingosine kinase are critical for transforming growth factor-beta-stimulated collagen production by cardiac fibroblasts. *Cardiovasc Res*. 2009;82:303–312.
38. **Oh SP, Seki T, Goss KA, et al.** Activin receptor-like kinase 1 modulates transforming growth factor-beta 1 signaling in the regulation of angiogenesis. *Proc Natl Acad Sci U S A*. 2000;97:2626–2631.
39. **Castañares C, Redondo-Horcajo M, Magán-Marchal N, ten Dijke P, Lamas S, Rodríguez-Pascual F.** Signaling by ALK5 mediates TGF-beta-induced ET-1 expression in endothelial cells: A role for migration and proliferation. *J Cell Sci*. 2007;120:1256–1266.
40. **Johnson DW, Berg JN, Baldwin MA, et al.** Mutations in the activin receptor-like kinase 1 gene in hereditary haemorrhagic telangiectasia type 2. *Nat Genet*. 1996;13:189–195.
41. **Abdalla SA, Pece-Barbara N, Vera S, et al.** Analysis of ALK-1 and endoglin in newborns from families with hereditary hemorrhagic telangiectasia type 2. *Hum Mol Genet*. 2000;9:1227–1237.